

ISSN-0011-1643

UDC 541.1

CCA-2064

Original Scientific Paper

Light Scattering from Polydispersed Fractal Clusters in Solution

Sow Hsin Chen

*Department of Nuclear Engineering and
Center for Materials Science and Engineering,
Massachusetts Institute of Technology, Cambridge, Mass. 02139, U.S.A.*

Jacques Rouch

Physics Department, C.P.M.O.H., University Bordeaux I,
351 Cours de la Liberation 33405 Talence Cedex France*

and

Pierro Tartaglia

*Dipartimento di Fisica, Università di Roma, »La Sapienza«,
Piazzale Aldo Moro 2, I-00185 Roma, Italy*

Received August 16, 1991

A brief review is given of our recent theoretical and experimental work on static and dynamic light scattering from aggregating polystyrene lattices in solutions and percolating dense microemulsions. The former is characterized by formation and growth of reaction limited fractal aggregates induced by addition of salt, and is basically a nonequilibrium phenomenon. The latter, however, is characterized by formation and growth of clusters of dynamically percolated microemulsion droplets, as one approaches the percolation threshold from below, and is an equilibrium phenomenon. Theories of static and dynamic light scattering from these polydispersed fractal clusters are formulated, emphasizing calculations of the universal scaling functions measurable in the experiment. Experimental data are then analyzed to substantiate the theoretical predictions. The similarity of the latter case with the well-known results from the equilibrium critical phenomena is pointed out.

* Centre de Physique Moléculaire Optique et Hertzienne is Unité. Associée 283 du C.N.R.S.

I. INTRODUCTION

In the last several years, the understanding of the kinetic processes which govern the aggregation of the colloidal particles and the structure of the resulting clusters have been the subject of considerable general interest.^{1,2,3} In particular, in recent experiments, a fractional power law dependence of the mass m on the size of the aggregates was found. It is well known that small particles can aggregate to form porous, low-density macroscopic clusters that behave quantitatively in a way different from ordinary bulk matter.⁴ The resulting structures are characterized by the fractal dimension D_f which relates a typical dimension of the aggregates to their masses. Quantitatively, the radius of gyration, defined as the second moment of the mass distribution according to:

$$R_g^2 = \frac{1}{m} \sum_{i=1}^k M_i r_i^2 \quad (1)$$

where \vec{r}_i is the distance from the center of mass of the i th particle, obeys the relationship:

$$R_g \approx m^{1/D_f} \quad (2)$$

This kind of aggregation process is relevant for a variety of colloidal and heterogeneous systems, including hydrophobic sols, micelles, microemulsions, liposomes, gels and foams. The connection between non-equilibrium growth and aggregation processes, with well defined scaling and universality properties, remains to be explained. Several theoretical models,¹⁻⁴ which provide realistic descriptions of the aggregation processes occurring in colloidal systems, have been developed recently.

In this paper, we discuss interpretation of measurements of the growing aggregates of polystyrene latex particles in solution, made by the dynamic light scattering technique. The use of colloidal suspension of charged particles in aqueous media offers the possibility that the physical properties of the suspension can be tuned easily by simply varying the ionic strength of the aqueous phase. Polymer lattices present a model colloidal systems due to the availability of monodispersed particles of suitable dimensions, convenient for light scattering experiments. We model the lattices in solution as a system of hydrophobic polystyrene spheres stabilized by double layer repulsions derived from adsorbed emulsifier ions or from sulfate endgroups of the polymer molecules. If the emulsifier is removed, or the thickness of the double layer reduced by adding an appropriate amount of a simple salt, the particles will lose their charges and aggregate to form large structures. The importance of this model system lies in the fact that different aggregation mechanisms, such as reaction limited or diffusion limited processes, can be realized by varying the external conditions. Moreover, if the charge groups are left in the H^+ form, conductometric titration⁵ with a base allows their number to be determined, giving a full characterization of particle charges.

Certain compositions of three-component mixtures of water, oil and ionic or non-ionic surfactants may form homogeneous, thermodynamically stable and optically transparent liquid phases known as microemulsions.⁶ The microemulsion, in the case of water/decane/AOT [sodium bis di-2-ethyl hexyl sulfosuccinate] system, consists of water droplets, coated by a monolayer of the surfactant, dispersed in the oil.⁷ The average size of the droplets is governed by the molar ratio $\omega = [H_2O]/[AOT]$. When ω is

equal to 40, the dimension of the droplet is of the order of 160 Å, which explains the fact that the solution is optically transparent. Nevertheless, the microemulsion scatters enough light to be observable by photon correlation spectroscopy.⁸ At constant pressure, upon changing the amount of oil, keeping the ω fixed, the volume fraction of the droplets can be varied continuously from a few percent to 90%, without changing the average size and size distribution of the droplets. On varying the temperature at a fixed volume fraction, the microemulsion system shows a variety of interesting physical phenomena including a binary phase separation having a consolute lower critical point for the volume fractions below 0.4,⁹ and an electrical percolation occurring over the whole range of the volume fractions at different temperatures.¹⁰ It has been shown that the electrical percolation phenomenon below the percolation threshold can be described by a dynamic percolation process in which the counterions migrate from droplet to droplet, owing to a strong mutual attraction, when the centers of the two droplets approach to within a certain distance.¹¹ Another transport coefficient, namely the viscosity of the microemulsion, also shows percolation behavior.¹² This indicates that, above the percolation threshold, the droplets show an increasing connectivity between them and the system evolves toward, possibly, a bicontinuous structure.

In this paper, we shall discuss the approach to the percolation threshold from below, studied by static and dynamic light scattering. Even though the functional form of the cluster sizes distribution remains the same, as governed by the percolation theory, the divergence of the average cluster size on approaching the percolation threshold has a profound effect in both the light scattering intensity and the droplet density-density time correlation function. An analytical theory will be presented for the calculations of these two quantities, in analogy with the aggregation problem.¹³ We will show that the essential difference, as far as the light scattering properties are concerned, between the aggregation problem and the percolation problem, lies in the fact that the polydispersity exponent τ has different values for the two cases. In the reaction limited aggregation problem, τ has a value 1.5 and is unrelated to the fractal dimension D_f of the cluster, which is found to be equal to 2.1. On the other hand, in the case of percolation, τ has a universal value 2.2 and is linked to the fractal dimension by a hyper-scaling relation² $D_f(\tau-1) = d$, leading to a fractal dimension $D_f = 2.5$ in three dimensions ($d=3$). For τ smaller than 2, the first cumulant in the dynamic light scattering shows a crossover from a q^2 to another q^2 behavior at a certain characteristic q value, while for τ greater than 2, the first cumulant shows an interesting crossover from a q^2 to a q^3 behavior at a certain characteristic q value related to the average cluster dimension.

II. GENERAL THEORY OF LIGHT SCATTERING FROM POLYDISPERSED FRACTAL AGGREGATES

Let us imagine scattering of light from an arbitrary cluster of k identical spherical particles of diameter R_1 . In the cases under study, the size of particles is such that R_1 is less than 500 Å. The Bragg wave number for scattering of a laser light of wave length λ from a medium of index of refraction n at a scattering angle θ , is given by $q = (4\pi n/\lambda)\sin\theta/2$. For a common light scattering setup using He-Ne laser and a scattering angle of 90° from a aqueous medium, $q = 1.87 \times 10^{-3} \text{ \AA}^{-1}$, and qR_1 is less than unity. Then, the particle form factor can be taken effectively equal to one. The scattering intensity due to a cluster of k particles is proportional to an interference factor

$\left\langle \left| \sum_{l=1}^{\infty} A_l \exp[i\vec{q} \cdot \vec{r}_l] \right|^2 \right\rangle$. This quantity is equal to Ak^2 at $q = 0$ for identical particles of scattering amplitude A . Thus, if we introduce an intra-cluster structure factor $S_k(q)$ which is normalized to unity at $q = 0$, then the light scattering intensity at small q can be written as:

$$I(q) = A^2 \sum_{k=1}^{\infty} N(k) k^2 S_k(q) \tag{3}$$

In this equation, $N(k)$ is the number of clusters with k particles, which is related to the total number of particles N in the scattering volume by $N = \sum_{k=1}^{\infty} k N(k)$. Thus, the scattering intensity at $q = 0$ is given by: $I(0) = N A^2 \langle k^2 \rangle / \langle k \rangle$ where the bracket denotes the average over the cluster size distribution function $N(k)$. It should be noted that in writing eq. (3), we make an implicit assumption that the cluster-cluster interference effect can be neglected in the calculation of the total scattered intensity. This assumption is certainly true of dilute systems. But, it can also be justified for dense systems in the following way. Since the scattered intensity is heavily weighted by the larger clusters and the larger clusters are presumably scattered around in the sea of smaller clusters, the system can be taken to be effectively dilute in this sense.

The calculation of the scattered intensity, therefore, reduces to specifying the intra-cluster structure factor $S_k(q)$ and the cluster size distribution function. For a fractal cluster of k particles and fractal dimension D_f , Chen and Teixeira¹⁴ have previously written an approximate intra-cluster structure factor. In the normalized form it can be written as:

$$S_k(q) = \frac{\sin [(D_f-1) \arctan(qR_k)]}{(D_f-1) qR_k (1+q^2R_k^2)^{\frac{D_f-1}{2}}} \tag{4}$$

In the above formula, R_k is the radius of gyration of the k -cluster. R_k and R_1 are connected by:

$$R_k = R_1 k^{1/D_f} \tag{5}$$

Two asymptotic forms, which will be extensively used in the next section, can be deduced from the structure factor given in equation (4).

For low values of qR_k , the structure factor can be approximated by:

$$S_k^{(1)}(q) \approx \exp[-D_f(D_f+1) q^2R_k^2/6] \tag{6}$$

On the other hand, for large values of qR_k , it takes the limiting form:

$$S_k^{(2)}(q) \approx \frac{\sin[(D_f-1)\pi/2] (qR_k)^{-D_f}}{(D_f-1)} \tag{7}$$

The cluster size distribution function $N(k)$ in both cases can be written in the following scaled form: $N(k) \propto k^{-\tau} f[(k/s)]$.² In this expression, the parameter s is a measure

of the number of particles in a typical cluster. For a fixed value of s , the exponent τ specifies the degree of polydispersity of the cluster sizes; the smaller the τ value, the broader the distribution. Remembering that the value of k starts from unity, the normalized form of the cluster size distribution function can be written as:

$$N(k) = \frac{s^{\tau-2}}{\Gamma\left(2-\tau, \frac{1}{s}\right)} k^{-\tau} \exp\left[-\frac{k}{s}\right] \quad (8)$$

where $\Gamma(a,b)$ is the incomplete Euler Gamma function.

The dynamic light scattering measures the particle density-density time correlation function, which can be computed according to the formula:

$$C(t) = \frac{\sum_{k=1}^{\infty} k^2 N(k) S_k(q) \exp[-D_k q^2 t]}{\sum_{k=1}^{\infty} k^2 N(k) S_k(q)} \quad (9)$$

The first cumulant can be calculated by taking the $t=0$ limit of the logarithmic derivative of $C(t)$

$$\Gamma_c(q) = \frac{\sum_{k=1}^{\infty} k^2 N(k) S_k(q) D_k q^2}{\sum_{k=1}^{\infty} k^2 N(k) S_k(q)} \quad (10)$$

The D_k in these equations is the effective cluster diffusion constant, including both the translational and rotational contributions. It can be approximately written as:¹⁵

$$D_k = D_1 k^{-1/D_f} \left[1 + \frac{1}{2\rho^2} \right] \quad (11)$$

where $D_1 = \frac{K_B T}{6 \pi \eta_s R_1}$ is the Stokes Einstein translational diffusion coefficient for a single particle, η_s is the viscosity of the solvent and ρ is the ratio of the hydrodynamic radius to the radius of gyration of the cluster.

III. THE SCALED SCATTERED INTENSITY AND CUMULANT

In practice, the summation over k in equations (3), (9), and (10) is replaced by an integral over k from 1 to infinity. In order to obtain analytical expressions, the structure factor has been taken to coincide with the two asymptotic forms (6) and (7), depending on whether the parameter qR_k is less or greater than one. Thus, the integration over k can be split into two ranges, one from 1 to k_0 and the other from k_0 to infinity, where $k_0 = (qR_1)^{-D_f}$. For example, the intensity is calculated as:

$$I(q) = \int_1^{(qR_1)^{-D_f}} dk N(k) k^2 S_k^{(1)}(q) + \int_{(qR_1)^{-D_f}}^{\infty} dk N(k) k^2 S_k^{(2)}(q) \tag{12}$$

The result of integration gives:¹³

$$I(x,s) = \frac{s}{\Gamma(2-\tau)} \left[F(3-\tau,x) [1+x^2]^{\frac{D_f(3-\tau)}{2}} + G(2-\tau,x) \left[\frac{x}{h} \right]^{-D_f} \right] \tag{13}$$

where $x = q\xi$ and the correlation length ξ is defined as $\xi = hR_1 s^{1/D_f}$. This quantity is very close to the average radius of gyration of the clusters. In eq (13), $F(a,x) = \Gamma(a) - \Gamma(a,u)$ with: $u = [h^2(1+x^2)/x^2]^{D_f/2}$; $h = [D_f(D_f+1)/6]^{1/2}$; and $G(a,x) = \sin[(D_f-1)\pi/2] \Gamma(a,(x/h)^{D_f})/(D_f-1)$.

Equation (13) can be reduced to simpler forms in two limiting cases:

a) For $x <$

$$I(x,s) = \frac{s}{\Gamma(2-\tau)} \Gamma(3-\tau) (1+x^2)^{-D_f(3-\tau)/2} \tag{14}$$

noting that $I(x=0,s) = I_0 = s\Gamma(3-\tau)/\Gamma(2-\tau)$.

b) For $x > 1$

$$I(x,s) = \frac{s}{\Gamma(2-\tau)} \left[F(3-\tau,\infty) x^{-D_f(3-\tau)} + \frac{\sin \left[\frac{(D_f-1)\pi}{2} \right]}{D_f-1} \Gamma(2-\tau) \left(\frac{x}{h} \right)^{-D_f} \right] \tag{15}$$

In the large q limit, applicable to neutron and X-ray scattering experiments, two different asymptotic forms can be observed, depending on the value of the polydispersity exponent τ . For the reaction limited aggregation (RLA), the exponent τ is known to be 1.5. In this case, the asymptotic behavior of the scattered intensity goes like: $I(x) \rightarrow (x)^{-D_f}$ giving directly the fractal dimension. On the other hand, for the percolation case, $\tau=2.2$, and the asymptotic intensity is $I(x) \rightarrow (x)^{-D_f(3-\tau)} = (x)^{-2}$, which does not give information on the fractal dimension. It should be remarked here that this asymptotic regime is an intermediate regime in q where one is probing the length scale of ξ . On further increase of q , the intensity would eventually approach the Porod regime $(q)^{-4}$ where the length scale of the size of the spheres is probed. In order to obtain this regime, the particle form facto has to be multiplied to the intensity formula given in equation (3).

The calculation of the cumulant can be similarly made starting from equation (10). Defining a reduced cumulant by $\Gamma_c^* = \Gamma_c/(D_1R_1q^3)$, one can show.¹³

$$\Gamma_c^*(x) = \frac{F\left(3-\tau-\frac{1}{D_f}, x\right)}{I(x,s)} [1+x^2]^{D_f(1-\tau-1/D_f)/2} + \left[1+\frac{1}{2\rho^2}\right] \frac{G\left(2-\tau-\frac{1}{D_f}, x\right)}{I(x,s)} \left[\frac{x}{h}\right]^{-D_f} \tag{16}$$

Again, two limiting cases can be identified. For $x \rightarrow 0$, Γ_c^* goes like $1/x$ according to:

$$\Gamma_c^*(x) \approx \frac{h}{x} \frac{\Gamma\left(3 - \tau - \frac{1}{D_f}\right)}{\Gamma(3 - \tau)} \quad (17)$$

but for large x limit, the two cases have different asymptotic behavior. For RLA we have:

$$\Gamma_c^*(x) \approx \frac{h}{x} \left(1 + \frac{1}{2\rho^2}\right) \frac{\Gamma\left(2 - \tau - \frac{1}{D_f}\right)}{\Gamma(2 - \tau)} \quad (18)$$

which shows a linear dependence on $1/x$. while for the percolation case, we have:

$$\Gamma_c^*(x) \approx h \frac{\Gamma\left(3 - \tau - \frac{1}{D_f}, \infty\right)}{\Gamma(3 - \tau, \infty)} \quad (19)$$

which is independent of x .

It is possible to cast the time correlation function $C(t)$ also into the scaled form, $C(x, v)$, where v is a natural non-dimensional scaled variable given by: $v = D_1 q^2 t s^{-1/D}$. The detailed expression is given in Reference [13]. It is sufficient here just to note that in the long time limit, the time correlation function approaches a stretched exponential form given by:

$$C(v) \approx \exp[-(D_f + 1) (v/D_f)^\beta] \quad (20)$$

where the stretch exponent β is universal and given by $\beta = D_f/(1+D_f)$. Thus, it can be seen that the droplet time correlation function starts off at short time as an exponential with a well defined first cumulant and tends, at long time, to a stretched exponential having an universal stretch exponent. The crossover from the exponential to the stretched exponential occurs at $\Gamma_c t = 1$.

IV. AGGREGATION OF POLYSTYRENE LATEX PARTICLES IN AQUEOUS SOLUTIONS

It has been shown by Cametti *et al.*¹⁶ that polystyrene lattices can be made to aggregate in aqueous medium by adding the simple salt NaCl. For example, for latex particles of 455 Å in deionized water, the addition of 0.17 mol/l of NaCl would result in irreversible reaction limited aggregation, with hydrodynamic radius of the typical cluster growing exponentially in time, with a time constant of about 5000 minutes. For light scattering experiments, a typical concentration of latex particles is about 5×10^{-5} in volume fraction. Recently, Lin *et al.*¹⁵ have experimentally shown that, for three completely different colloids, namely gold, silica, and polystyrene particles, a universal behavior of the reaction limited aggregation exists. According to these authors, for RLA clusters the fractal dimension D_f is equal to 2.10 ± 0.05 , and the polydispersity exponent $\tau = 1.50 \pm 0.05$. The fractal dimension D_f can be best determined by a combined

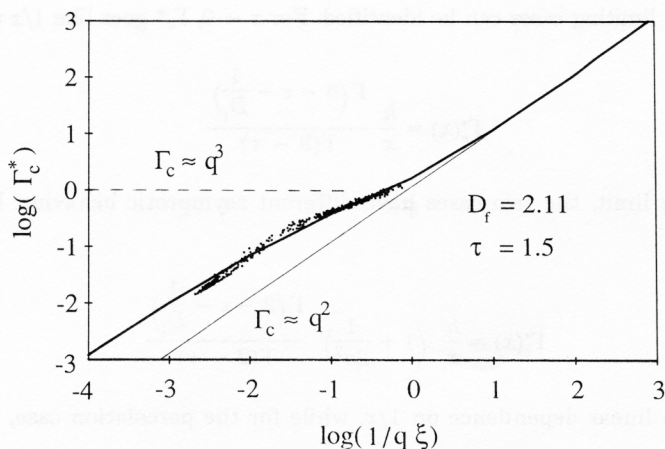


Figure 1. A plot of the reduced cumulant Γ_c^* vs. $1/x$ in a log-log scale for an aggregating polystyrene latex sphere of radius 455 Å in deionized water upon addition of 0.17 mol/l of NaCl. The correlation length $\xi = h R_1 s^{1/D_f}$ and the typical cluster size $s(t)$ grows exponentially in time with a time constant of about 5000 minutes.

static light scattering and X-ray small angle scattering using equation (15), as it was originally shown by Schaefer *et al.*¹⁷. This was possible because the polydispersity exponent τ is significantly smaller than 2. When τ is above 2 as for the case of percolation, the slope obtained by plotting $\log I(q)$ vs. $\log(q)$ would not give the correct fractal dimension, as it can be clearly seen from equation (15). Knowing that $D_f = 2.1$, one can then proceed to show by using dynamic light scattering that the exponent τ has a value 1.5.

If one plots the logarithm of the reduced first cumulant, $\log(\Gamma_c^*)$, vs. $\log(1/x)$, then equation (16) will give a solid line shown in Figure 1.¹⁸ It can be seen from the asymptotic formulae (equations (17) and (18)) that the universal scaling curve for the reduced cumulant vs. $\log(1/x)$ should show a slope of unity at high x and also a slope of unity at low x , with a crossover occurring at approximately $x = 10$. The absolute level of the universal plot is sensitive to the magnitude of τ . In this figure, the solid line has been drawn by assuming $\tau = 1.5$. In the same figure, dynamic light scattering data, taken from solutions having different salt concentrations, have been plotted as solid circles. It is striking to see that the experimental data span the region of crossover and agree well with the theoretical predictions.

In Figure 2,¹⁸ the solid lines are plots of $\ln[-\ln(C(v))]$ vs. $\ln[v]$ where the photon correlation function $C(v)$ is calculated according to equation (9) assuming $D_f = 2.11$ and $\tau = 1.5$. At large v , the time correlation function tends to a stretched exponential with a stretched exponent β calculated according to $\beta = D_f/(1+D_f)$. In Figure 2, the slope of the lines at the upper end is 0.68 as predicted by equation (20). Solid circles represent experimental data. The ξ value has to be determined by knowing the time dependence of $s(t)$. In this case, it is known that the cluster size grows exponentially in time, so that an empirical form $s(t) = s_0 \exp(at)$ is used. The parameters s_0 and a are separately determined at each salt concentration. It is again noted that most of

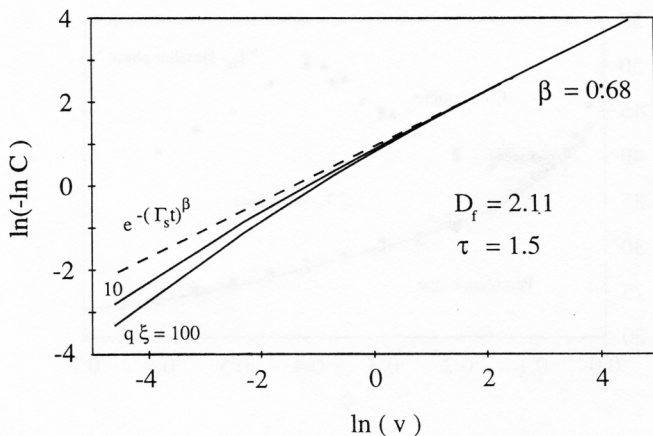


Figure 2. Double log of the photon correlation function plotted as the logarithm of the scaled time $\nu = D_1 q^2 t s^{-1}/D_f t$ for the same system of aggregating polystyrene latex particles as in Figure 1. The solid lines are theoretical predictions and the dots are experimental points. It should be noted that the asymptotic region where exponent b can be determined is experimentally very hard to reach.

the time correlation functions are taken at the crossover range so that the determination of β is difficult in practice.

V. PERCOLATING DENSE AOT/WATER/DECANE MICROEMULSIONS

Many three-component water-in-oil ionic microemulsions show the percolation phenomenon as a function of temperature at a constant volume fraction of the dispersed phase. As the temperature is increased from below the percolation threshold T_p , the low frequency conductivity σ increases sharply near T_p and can be described by a power law divergence $\sigma = \text{const} \times (T_p - T)^{-s'}$ where the dynamic percolation exponent has a value $s' = 1.2 \pm 0.1$.¹⁰ The conductivity far below the threshold (say 10 °C away) can be well described by a formula $\sigma = \phi \epsilon \kappa B T / (8\pi^2 \eta r^3)$, where ϕ is the volume fraction of the droplets of radius r , ϵ and η are, respectively, the dielectric constant and the shear viscosity of the oil. This expression follows from a charge fluctuation model of Eicke and Borkovec¹⁹ in which the mechanism of charge transport is attributed to the transfer of ionic species, either the surfactant molecules or their counterions. The migration of charged species from droplet to droplet produces a mean square charge fluctuation $\langle (ez)^2 \rangle$, which is calculated by applying a thermodynamic fluctuation theory in conjunction with Born's theory of ionic solvation. The conductivity is then obtained by calculating the mobility of a charged sphere of radius r carrying a mean square charge $\langle (ze)^2 \rangle$. Above the percolation threshold, the conductivity further increases towards the value of the aqueous phase in a power law fashion according to $\sigma = \text{const.} \times (T - T_p)^t$ with the static percolation index $t = 1.9 \pm 0.1$.¹⁰

AOT/Water/Decane three-component ionic microemulsion has a special feature of interest owing to the existence of a well defined percolation locus in the $T-\phi$ phase diagram. Referring to Figure 3, the percolation line cuts through the phase diagram from 40 °C at a volume fraction 0.08 down to 23 °C at a volume fraction $\phi = 0.65$.

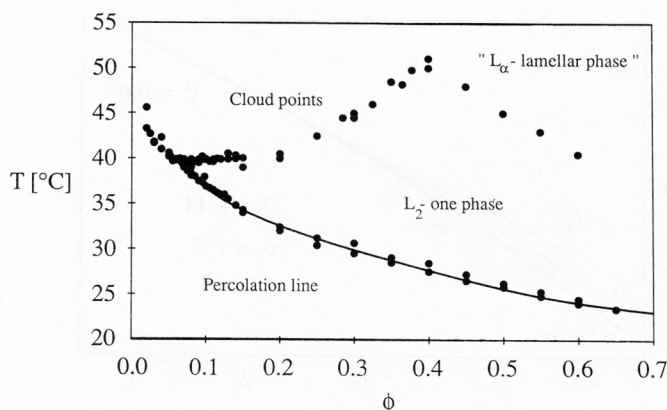


Figure 3. T - ϕ phase diagram of AOT/water/decane system at $\omega = 40.8$. The solid line is the percolation locus as determined by electrical conductivity measurements.

This means that one can approach the percolation threshold from below by keeping the volume fraction constant and increase the temperature or keeping the temperature constant and increase the volume fraction. The basic percolation phenomena observed in the two paths of approach are the same. We shall describe the results of light scattering experiments taking the latter path keeping the temperature at 23.5 °C and 25 °C.²¹

A. Light Scattering Intensity

The basic theoretical prediction is equation (13). Taking the value of polydispersity exponent τ equal to 2.2 from percolation theory, and the fractal dimension $D_f = 2.5$ as implied by the hyper-scaling relation $D_f(\tau-1) = 3$, the intensity in the region where $x = q\xi$ is small as compared to one, is predicted by the theory (*cf.* equation 14) to be:

$$I(x < 1) \approx \frac{\xi^{D_f}}{(1 + x^2)^{\frac{D_f}{2}(3 - \tau)}} \quad (21)$$

This means that $I(x)$ diverges at small q like ξ^{D_f} . This is shown in the inset of Figure 4 where we plotted the measured intensity data $I(x)$ as a function of q at a temperature 25 °C and a set of volume fractions ranging from 0.05 up to 0.58. From fitting the curves using equation (21), we get:

$$\xi = \xi_0 (\phi_p - \phi)^{-\nu} \quad (22)$$

where ξ_0 is 257 Å, $\phi_p = 0.59$, and the exponent $\nu = 0.88$, which is consistent with the percolation theory.²¹ The value of ξ_0 is of the order of the droplet size which is 180 Å and the value of the percolation threshold ϕ_p agrees with the percolation locus depicted in Figure 3. In the same graph, we also show that $I(x)/I_0$ is an universal function of x , following equation (13), which is the solid line and the experiment data are taken from reference.²¹

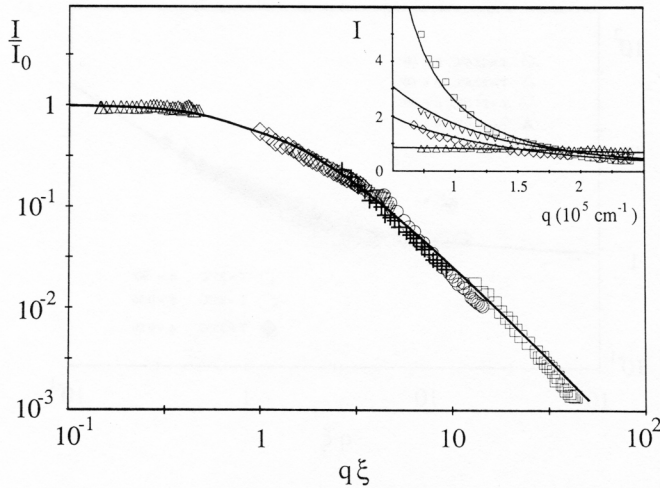


Figure 4. Scaling plot of the reduced scattered intensity *vs.* the scaling variable $x = q\xi$. Solid line is equation (13) and the symbols are experimental points from reference 21. In the inset, we show the low angle scattered intensities *vs.* q for volume fractions ranging from 0.05 to 0.58 taken from reference [21]. The solid lines are the relations given by equation (21).

B. The First Cumulant

The first cumulant of the droplet density-density correlation function is the easiest quantity to measure in a dynamic light scattering experiment and therefore is the most accurate quantity to be determined. We focus attention on the reduced cumulant $\Gamma_c^* = \Gamma_c / (D_1 R_1 q^3)$. As noted before, equation (16) is the complete form of the scaled first cumulant. At low value of the scaling variable x, Γ_c^* is proportional to $1/x$, according to equation (17). This regime corresponds to the solid line with a slope of unity appearing on the right hand part of Figure 5. On the other hand, at large values of x , the scaled first cumulant is independent of x (see equation 19). This regime corresponds to the horizontal line drawn on the left hand side of the Figure 5. It should be noted that this latter feature is in sharp contrast to the behavior described for the aggregation problem in the previous section. The symbols in Figure 5 are taken from published experimental data of Sheu *et al.*²⁰ taken at 22.6 °C and Magazù *et al.*²¹ taken at 25 °C. It should be observed that the theoretical prediction of transition of Γ_c from the q^2 behavior at small x to a q^3 behavior at large x , is well substantiated by the experimental data.

C. The Droplet Density Correlation Function

The main theoretical prediction for the time correlation function is that it begins with an exponential decay at short time with a well defined cumulant and gradually evolves into a stretched exponential decay at long time with an universal stretched exponent $\beta = 0.714$. The theoretical prediction can be summarized by a set of curves in Figure 6, where $\ln(-\ln(C))$ is plotted as a function of $\ln(\Gamma_c t)$, for different values of dimensionless parameter $q\xi$. We see from the solid lines that these universal curves all start with a slope of unity at small values of t and cross over to another slope β at

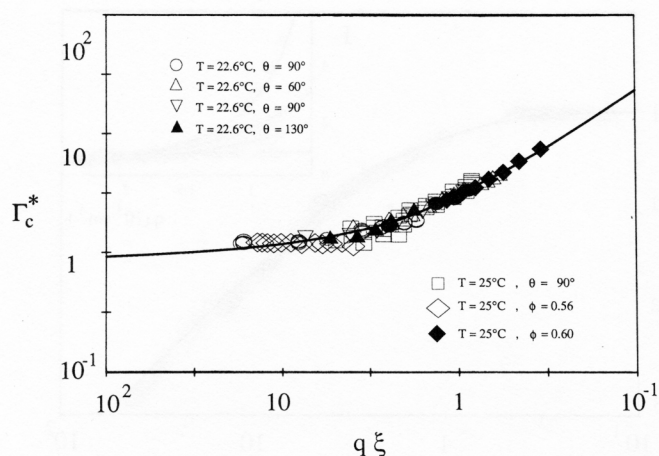


Figure 5. Scaling plot of the reduced first cumulant *vs.* the scaling variable $x = q\xi$. Note that the experimental data clearly indicate the transition from a linear behavior to a constant as the percolation threshold is approached.

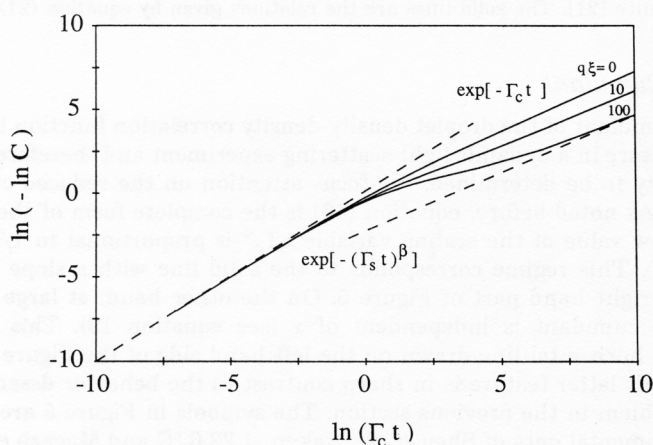


Figure 6. Double log of the droplet density time correlation function *vs.* the logarithm of $\Gamma_c t$ for different values of x . The crossover from a linear (single exponential decay) to another linear behavior (stretched exponential) takes place around $\Gamma_c t = 1$. Note again that asymptotic region is very hard to reach experimentally.

large values of t . The crossover occurs at approximately $t = 1/\Gamma_c$ depending on the values of $q\xi$. In practice, this crossover happens at about 1 ms. Thus, in order to obtain the precise value of β , one has to measure the time correlation functions starting from microsecond range to several seconds. The correlation functions decay to the background level at a time of the order of 100 milliseconds, making the determination of exponent β extremely difficult. Nevertheless, this universal curve has been tested against experimental data by Tartaglia *et al.*¹³ and was proven to be valid. The earlier

experiment and analysis by Sheu *et al.*²⁰— indicating a continuously changing β as functions of q and volume fraction was due to the fact that the correlation functions were largely taken at the crossover region where they had not reached the asymptotic form given by eq. (20).

VI. CONCLUSION

In this article we have shown that static and dynamic light scattering data from both reaction limited colloidal aggregates and percolating droplet microemulsions can be analyzed in a common and general way. Due to the fractal nature of the aggregates formed in both cases, the theory requires as an input the cluster size distribution function $N(k)$ given by equation (8) and the intra-cluster structure factor $S_k(q)$ given by equation (4). Two exponents, τ and D_f , enter into these two central quantities. In the former case, τ has a value 1.5 and D_f a value 2.1 and the two are unrelated. In the latter case, τ has a value 2.2 and D_f a value 2.5, the two being connected by the hyper-scaling relation. The physics of the RLA is controlled by the fact that the typical cluster size $s(t)$ grows exponentially in time when salt is added. On the other hand, the physics of the percolating microemulsion is controlled by the growing cluster dimension ξ as the percolation threshold is approached. This latter fact brings the physics of percolating microemulsions closer to the equilibrium critical phenomena.²³ We see, for example, that the q dependence of the scattered intensity obeys a relation similar to the Ornstein Zernike relation, with the intensity at $q = 0$ diverging like ξ^{D_f} and the q dependence of the first cumulant of dynamic light scattering changing from q^2 to q^3 as the percolation point is approached, much the same as in the equilibrium critical phenomena. What remains to be seen and explained is why the density time correlation function, although decaying exponentially initially in both cases, crosses over to the stretched exponential at the long time in the case of percolating microemulsions, was not also observed in critical phenomena.

Acknowledgement. — The authors wish to thank Dr. Ď. Težak for the suggestion of writing this short review article. SHC is grateful to the Physics Department of the University Bordeaux I for awarding a Visiting Professorship, during which this article was completed. This research is supported by DOE PE-FG01-91ER45429.

REFERENCES

1. D. P. Landau and F. Family, Eds., *Kinetics of Aggregation and Gelation* North Holland, Amsterdam 1984.
2. H. E. Stanley and N. Ostrowsky, Eds, *On Growth and Form* Nijhoff, Dordrecht, 1986.
3. R. Pynn and A. Skjeltorp, Eds., *Scaling Phenomena in Disordered System*, Plenum, N.Y. 1986.
4. J. Feder, *Fractal*, (Plenum, New York, 1988).
5. H. J. van den Hull and J. W. Vanderhoff, *J. Electroanal. Chem.* **37** (1972) 161.
6. S. H. Chen and R. Rajagopalan, *Micellar Solutions and Microemulsions-Structure, Dynamics and Statistical Thermodynamics*, Springer Verlag, New York (1990).
7. S. H. Chen, T. L. Lin, and J. S. Huang, in *Physics of Complex and Supramolecular Fluids*, edited by S. Safran and N. A. Clark (Wiley, New York, 1987).
8. S. H. Chen and J. S. Huang, *Phys. Rev. Lett.* **55** (1985) 1888.
9. M. Kotlarchyck, S. H. Chen, J. S. Huang, and M. W. Kim, *Phys. Rev.* **A29** (1984) 2054; J. Rouch, A. Safouane, P. Tartaglia, and S. H. Chen, *J. Chem. Phys.* **90** (1989) 3756; J. Rouch, A. Safouane, P. Tartaglia, and S. H. Chen, *J. Phys.* **C1** (1989) 1773.

10. C. Cametti, P. Codastefano, P. Tartaglia, J. Rouch, and S. H. Chen, *Phys. Rev. Lett.* **64** (1990) 1461; C. Cametti, P. Codastefano, A. Di Biasio, P. Tartaglia, and S. H. Chen, *Phys. Rev.* **A40** (1989) 2013.
11. G. S. Grest, I. Webman, S. A. Safran, and A. R. L. Bug, *Phys. Rev.* **A33** (1986) 12842
12. D. Majolino, F. Malamace, S. Venuto, and N. Micali, *Phys. Rev.* **A42** (1990) 7330.
13. P. Tartaglia, J. Rouch, and S. H. Chen, *Light Scattering from Dense Percolating Microemulsions*, to be published in *Phys. Rev. A*, 1992.
14. S. H. Chen and J. Teixeira, *Phys. Rev. Lett.* **57** (1986) 2583.
15. M. Y. Lin, *Phys. Rev.* **A41** (1990) 2005; J. E. Martin, J. Wilconson, and J. Odinek, *Phys. Rev.* **A43** 1991 858.
16. C. Cametti, P. Codastefano, and P. Tartaglia, *Phys. Rev.* **A36** (1987) 4916; C. Cametti, P. Codastefano, and P. Tartaglia, *J. Colloid Interface Sci.* **131** (1989) 409.
17. D. W. Schaefer, *Phys. Rev. Lett.* **26** (1984) 2371.
18. C. Cametti, P. Codastefano, A. Di Biasio, and P. Tartaglia, to be published.
19. H. F. Eicke, M. Borkovec, and B. Das-Gupta, *J. Phys. Chem.* **93** (1989) 314.
20. E. Y. Sheu, S. H. Chen, J. S. Huang, and J. C. Sung, *Phys. Rev.* **A39** (1989) 5867.
21. S. Magazü, D. Majolino, G. Maisano, F. Malamace, and N. Micali, *Phys. Rev.* **A40** (1989) 2643.
22. D. Stauffer, *Phys. Rep.* **54** (1979) 1.
23. K. Kawasaki, *Ann Phys. (N.Y.)* **61** (1970) 1; S. M. Lo and K. Kawasaki, *Phys. Rev.* **A8** (1973) 2176.

SAŽETAK

Raspršenje svjetla na polidisperznim fraktalnim nakupinama

S. H. Chen, J. Rouch i P. Tartaglia

Načinjen je kratki pregled našega dosadašnjeg teorijskog i eksperimentalnog rada na statičkom i dinamičkom raspršenju svjetla na polistirenskim lateksima, koji agregiraju u otopinama, te rada na gustim mikroemulzijama u kojima se javlja perkolacija. Agregacija je karakterizirana nastajanjem i rastom reakcijski limitiranih fraktalnih agregata, induciranih dodatkom soli; u osnovi ona je neravnotežna pojava. Perkolacija je, pak, karakterizirana nastajanjem i rastom nakupina dinamički perkoliranih mikroemulzijskih kapljica kada se približava perkolacijskom pragu odozdo; to je ravnotežna pojava. Formulirane su teorije statičkog i dinamičkog raspršenja svjetla na takvim polidisperznim fraktalnim nakupinama, pri čemu je osobita pažnja posvećena izračunavanju univerzalnih skalnih funkcija mjerljivih u eksperimentu. Analizirani su eksperimentalni podaci da bi se potkrijepila teorijska predviđanja. Naglašena je sličnost posljednjeg slučaja s dobro poznatim rezultatima ravnotežnih kritičnih pojava.